A FDTD HYBRID "$M3d_{24}$-YEE" SCHEME WITH SUBGRIDDING FOR SOLVING LARGE ELECTROMAGNETIC PROBLEMS

Hany E.Abd El-Raouf*, Esam A.El-Diwani*, Abd El-Hadi Ammar, and Fatma M.El-Hefnawi ***

*Dept. of Microwave Engineering, Electronics Research Institute,Dokki,Cairo,Egypt.

**Faculty of Engineering, Al-Azhar University, Cairo, Egypt.

ABSTRACT- A hybrid scheme consisting of a modified second order in time- fourth order in space finite-difference time-domain (FDTD) scheme "$M3d_{24}$" and the Yee algorithm, with subgridding is introduced to overcome the errors of applying the 4th order in space FDTD at the interfaces of perfect electric conductors (PEC) or dielectric scatterers. This hybrid scheme is based on applying the Yee algorithm in the vicinity of the scatterer using a high resolution grid (number of points per wavelength), and the $M3d_{24}$ scheme in the other regions using a low resolution grid in order to reduce the required computer storage for large problems, while still good accuracy. The results of this hybrid scheme are shown to agree well with the results of the Yee algorithm using a high resolution grid, for problems of plane wave scattering from PEC cubes, spheres.

KEYWORDS

FDTD, higher order FDTD, resolution of the grid, subgridding, transient scattering of electromagnetic waves.

1. INTRODUCTION

Higher order FDTD algorithms are used to improve the accuracy of the computations when using a relatively low resolution grid. Taflove [1] approximated the derivatives in the conventional fourth order FDTD using the second order central difference in time and fourth order in space. A modified second order in time- fourth order in space FDTD scheme "$M3d_{24}$", has been deduced by the authors in [2,3,4]. The algorithm enables the numerical phase velocity error to be minimized, so that it leads to high accuracy with low resolution grids. The application of 4th order algorithms directly in the vicinity of a PEC or a dielectric scatterer introduces errors due to using large stencils in the 4th order algorithms [5,6]. Other sources of error are the large variations of the fields in the vicinity of an edge of a PEC or a large curvature of a surface of a PEC, that can not be reproduced with low resolution. To overcome the error of large stencils, Hadi [5] applied the 2nd order Yee algorithm in the vicinity of the scatterer, however, the Yee algorithm produces a significant error if it is applied using low resolution.

The approach adopted in this paper depends on the application of the Yee algorithm in the vicinity of the scatterer using a high resolution grid, and using the $M3d_{24}$ scheme with low resolution in the other regions to reduce the required storage for large problems. The high resolution is also required to reproduce fast variations of the fields in certain regions. In addition, complex structures which contain fine details in some regions need high resolution grids, whereas a 4th order scheme with low resolution can be applied in the remaining regions. A number of examples are given in the present paper to show the applicability of the scheme for different categories of problems.

2. METHOD OF SOLUTION

The modified 3D 4th order FDTD scheme "$M3d_{24}$" is introduced by the authors in [2,3,4]. The updating equations of the $M3d_{24}$ scheme have been derived as applications of a version of Ampere's law and Faraday's law using 2nd order central difference in time and 4th order in space.

The updating equation of the filed component E_x is,

$$
\begin{aligned}
E_x\Big|_{i,j,k}^{n+1} &= E_x\Big|_{i,j,k}^{n} + K_1 N_e (H_z\Big|_{i,j+1/2,k}^{n+1/2} \\
&- H_z\Big|_{i,j-1/2,k}^{n+1/2} - H_y\Big|_{i,j,k+1/2}^{n+1/2} \\
&+ H_y\Big|_{i,j,k-1/2}^{n+1/2}) + K_3 N_e (H_z\Big|_{i+1,j+1/2,k}^{n+1/2} \\
&- H_z\Big|_{i+1,j-1/2,k}^{n+1/2} + H_z\Big|_{i-1,j+1/2,k}^{n+1/2} \\
&- H_z\Big|_{i-1,j-1/2,k}^{n+1/2} - H_y\Big|_{i+1,j,k+1/2}^{n+1/2} \\
&+ H_y\Big|_{i+1,j,k-1/2}^{n+1/2} - H_y\Big|_{i-1,j,k+1/2}^{n+1/2} \\
&+ H_y\Big|_{i-1,j,k-1/2}^{n+1/2}) + \frac{K_2 N_e}{3} (H_z\Big|_{i,j+3/2,k}^{n+1/2} \\
&- H_z\Big|_{i,j-3/2,k}^{n+1/2} - H_y\Big|_{i,j,k+3/2}^{n+1/2} \\
&+ H_y\Big|_{i,j,k-3/2}^{n+1/2}) + \frac{K_4 N_e}{3} (H_z\Big|_{i+1,j+3/2,k}^{n+1/2} \\
&- H_z\Big|_{i+1,j-3/2,k}^{n+1/2} + H_z\Big|_{i-1,j+3/2,k}^{n+1/2}
\end{aligned}
$$

$$-H_z\Big|_{i-1,j-3/2,k}^{n+1/2} - H_y\Big|_{i+1,j,k+3/2}^{n+1/2} + H_y\Big|_{i+1,j,k-3/2}^{n+1/2} - H_y\Big|_{i-1,j,k+3/2}^{n+1/2} + H_y\Big|_{i-1,j,k-3/2}^{n+1/2} \quad (1)$$

where each point in the Yee cell $P(x_i, y_j, z_k) = P(ih, jh, kh)$ and the time $t_n = n\Delta t$, h and Δt are the space and time increments, i, j, k, n are integers and $N_c = \dfrac{\Delta t}{\varepsilon_0 h}$.

where the following conditions must be satisfied.

$$K_1 + K_2 + 2(K_3 + K_4) = 1 \quad (2)$$

$$\frac{K_4}{K_2} = \frac{K_3}{K_1} \equiv \frac{1 - (K_1 + K_2)}{2\ (K_1 + K_2)} \equiv \beta \quad (3)$$

The constants K_1, K_2, K_3 and K_4 are optimized to minimize the dispersion error in all directions at a certain frequency [3]. The time step Δt should be small w.r.t the cell size according to the stability condition [3],

$$\Delta t \le \frac{h}{\sqrt{3}c} \frac{1}{\left|1 - 2\beta \| K_1 - K_2 / 3\right|} \quad (4)$$

The other five E,H field components have a similar form corresponding to Ampere's and Faraday's laws in the different directions with the field locations conforming to the Yee cell. The magnetic field components are updated at times shifted by $\Delta t / 2$ w.r.t the times of the electric field components.

The present approach is based on applying the $M3d_{24}$ scheme using a coarse grid in the regions which are not in the vicinity of objects, and applying the Yee algorithm using a fine grid in a region that contains the object or the objects. The ratio of the resolution of the fine grid to that of the coarse grid to be used equals odd integers. An important property of using an odd integer ratio is that it provides colocated fields in space for the fine grid with the coarse grid (see Figure 1) [7]. The time step used is entirely constant in the domain with $\Delta t < \Delta t_{f\max}$ (where $\Delta t_{f\max}$ is the maximum allowable time step satisfying the stability condition in the fine grid).

At each time step the fields are updated in the coarse grid using $M3d_{24}$, then the tangential E-fields and the normal H-fields on the interface planes of the fine grid are interpolated from the coarse grid to the fine one. Finally the fields are updated in the fine grid using the Yee algorithm.

Assume that the electric and magnetic fields are denoted by $(\overline{E}, \overline{H})$ in the coarse grid and $(\overline{e}, \overline{h})$ in the fine grid. At a common point on the two grids with indices (i, j, k) on the coarse grid and (i', j', k') on the fine grid, the field $E_x(i, j, k)$ corresponds to the field $e_x(i'+1, j', k')$ (noting that the position of $E_x(i, j, k)$ is the point $((i + 1/2)\Delta x, j\Delta y, k\Delta z)$, Figure (1a)). The other five field components, $E_y(i, j, k)$ corresponds to $e_y(i', j'+1, k')$, $E_z(i, j, k)$ corresponds to $e_z(i', j, k'+1)$, $H_x(i, j, k)$ corresponds to $h_x(i', j'+1, k'+1)$, $H_y(i, j, k)$ corresponds to $h_y(i'+1, j', k'+1)$ and $H_z(i, j, k)$ corresponds to $h_z(i'+1, j'+1, k')$.

In order to show the actual steps of evaluations and interpolations of the fields in the coarse and the fine grids, we consider the x-component of the electric-field E_x and e_x. Assume the six boundary planes of the fine grid region (intersection planes between the fine and coarse grids) are $x_1 = i_{1b}\Delta x$, $x_2 = i_{2b}\Delta x$, $y_1 = j_{1b}\Delta y$, $y_2 = j_{2b}\Delta y$, $z_1 = k_{1b}\Delta z$ and $z_2 = k_{2b}\Delta z$ with $i_{2b} > i_{1b}$, $j_{2b} > j_{1b}$ and $k_{2b} > k_{1b}$. The steps of the computations will be as follows for each time step;

(1) E_x is updated in the coarse grid and in the intersection planes, i.e. in the region $\{(i_{2b} \le i < i_{1b})$ or $(j_{2b} \le j \le j_{1b})$ or $(k_{2b} \le k \le k_{1b})\}$, using $M3d_{24}$.

(2) E_x is interpolated on the four planes, the xy planes $z_1 = k_{1b}\Delta z$ and $z_2 = k_{2b}\Delta z$ and the xz planes $y_1 = j_{1b}\Delta y$ and $y_2 = j_{2b}\Delta y$ to find e_x on these planes. The interpolations on the xy plane $z_1 = k_{1b}\Delta z$ (Figure 1), can be evaluated as follows;
i)Linear interpolation is used to find the interpolated value of E_x at the points (p) in Figure1a, which are the positions of the e_x field at the same points (i,j,k) of E_x.
ii)The interpolated four field components $e_{x1}, \ldots\ldots, e_{x4}$ are used to obtain the fields at the points (x) (Figure 1b) using quintic interpolation.

(3) The e_x field is updated in the fine grid using the Yee algorithm.

(4) After updating the e_x field, the values of E_x are updated as $E_x = e_x$ at the common points of the low resolution and the high resolution grids in the domain of the fine grid.

(5) Simililar steps are to be repeated for the H field components.

The use of the Yee algorithm in the fine grid, rather than using the $M3d_{24}$ algorithm, has the obvious advantage that the

Yee algorithm does not have a large stencil thus it introduces only small errors at the object boundary. In addition, the use of high resolution will increase the accuracy of the Yee algorithm to the required value while using fewer floating point operations than the $M3d_{24}$ algorithm. Third, the time step $\Delta t_{f_{\max}}$ of the Yee algorithm is longer than the corresponding time step for $M3d_{24}$ (according to the stability condition of the two schemes [1], Eq.(4)), i.e. using $M3d_{24}$ in the fine grid will increase the required time steps to solve the problem.

3. REFLECTION ERROR OF SUBGRIDDING

Using multi-resolution grids in the computational domain introduces spurious reflections at the interfaces between the coarse grid and the fine one. These reflections are evaluated using a rectangular waveguide as discussed in [7], but our test is applied for the three-dimensional case. A TE_{10} mode, Gaussian pulse-modulated sine wave is excited at one end of a waveguide with a cross section of dimensions 20×9 mm and its center lies at the point (x_0, y_0). The total field is updated taking into consideration the boundary condition of the perfect conductor of the waveguide. The coarse grid has a cell edge length $h = \Delta x = \Delta y = \Delta z$ =1mm. The waveguide is long enough to eliminate reflections from the absorbing boundary condition (ABC). The modulated pulse is given by

$$g(t)= \sin 2\pi f_0 t \; e^{-(t/\tau)^2}, \qquad (5)$$

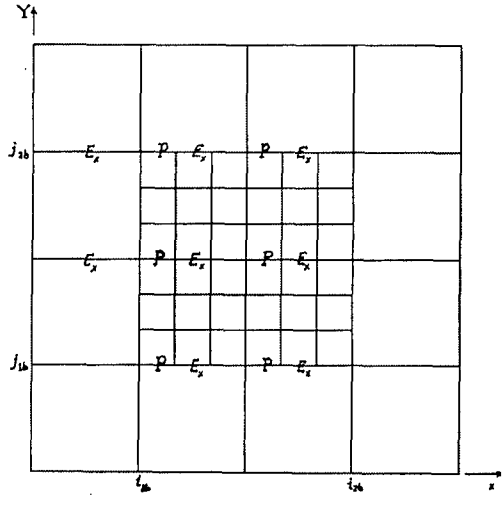

(a)

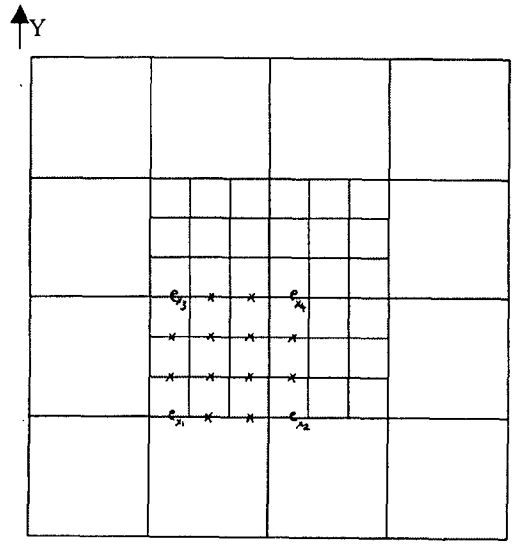

(b)

Figure 1. Steps of interpolations to find e_x from E_x in the planes z=$k_{1b}\Delta z$ or z=$k_{2b}\Delta z$. (a) Interpolation of the field values at the points (p), (b) the interpolated values e_{x1}, e_{x2}, e_{x3} and e_{x4} are used to obtain the field values at the points (x).

$f_0 = 1.5 f_{c_{1,0}}$ =11.25 GHZ,

$$\frac{1}{2\tau} = 20 \; GHZ \qquad (6)$$

where $f_{c_{1,0}}$ is the cuttoff frequency of the TE_{10} mode.

A fine grid region, with dimensions $16\times4\times40$ mm and cell edge length $\overline{h} = \overline{\Delta x} = \overline{\Delta y} = \overline{\Delta z}$ =1/3mm, is placed such that its center lies in the transverse plane at the point (x_0, y_0). It is to be noted that the reflections are due to all six interfaces of the subgridded region similar to the test region of Okoniewski et al [8], which must be greater than the reflections from the 2-dimensional test structure of Chevalier et al [7] in which the fine grid filled the entire second half of the waveguide.

The electric field component E_y is computed in front of the subgridded region and time steps are taken such that all reflections from the subgridded boundaries are taken into consideration. These time steps are stopped before any reflections return from the ABC. The same computations are repeated using entirely the coarse grid, i.e. without subgridding, and the resulting field values are taken as reference values. The difference in E_y between the two cases represents the reflected field from the interfaces of the subgridded region. Figure 2a shows the reflection coefficient in front of the subgridded region at the centeral point (x_0, y_0) in the transverse plane. Figure2b shows the reflection coefficient as an average of the reflection coefficients for different x-positions in front of the subgridded region in the transverse plane. The reflection coefficients in Figures 2a and 2b are plotted versus frequency from 7GHZ to

43GHZ (for resolution R=7 in the coarse grid). The subgridded zone is expected to yield multiple reflections along its length (40mm) as a half wavelength (corresponding to 3.75GHZ). Peaks at approximately multiples of this frequency are expected to occur, Figures 2a and 2b. At the lower end of the frequency the resolution is high and the waveguide approaches its cut off frequency which leads to lower reflections. It is seen from Figure 2 that the reflection coefficient in this frequency band lies below -35dB and for resolution $R \geq 10$ ($f \leq 30$GHZ) the reflection coefficient is smaller than -47dB.

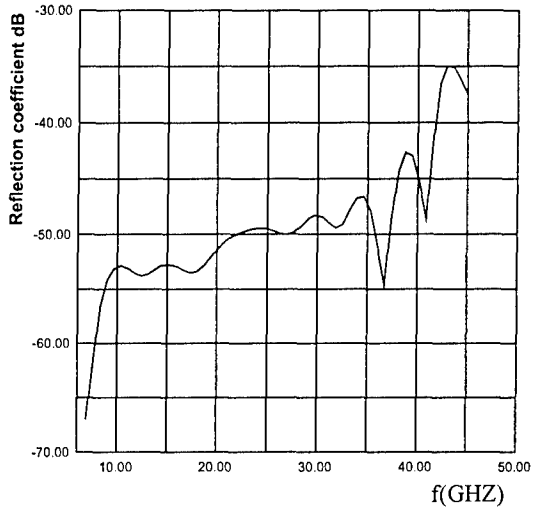

(a)

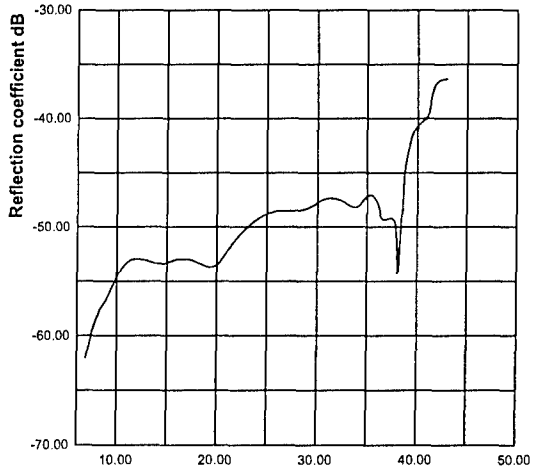

(b)

Figure 2. Reflection coefficient from a subgridded region 16 x 4 x 40 mm in a recatangular waveguide with coarse grid $\Delta x = \Delta y = \Delta z = 1\,mm$ and refinement factor 3. (a) Reflection coefficient at the centeral point of the transverse plane in front of the subgridding region, (b) average of the reflection coefficients for different x-positions in the transverse plane.

4. APPLICATION OF THE HYBRID SCHEME TO THE FAR FIELD CALCULATION FROM PLANE WAVE SCATTERING FROM PEC OBJECTS

The hybrid scheme is tested for the problem of scattering from PEC cubes and spheres to long distances to show the improvement of the accuracy compared with the Yee algorithm. Hadi [6,5] applied the 2nd order Yee algorithm in the vicinity of the PEC using a single resolution in the entire domain. The application of the Yee algorithm with low resolution, such as R=5, introduces a significant error[5].

The scattering from a cube is a good test to show the applicability of the scheme in the vicinity of PEC scatterers which contain edges. The scattering to a long distance shows the low dispersion error of the scheme. The backscattered electric field from a cube, with side length of 2.4λ, is plotted in Figure 3 with the distance from the cube. The low resolution (R=5) results of various schemes are compared with the high resolution (R=20) result of Yee algorithm. It is seen from Figure 3a that the application of the Yee algorithm with low resolution R=5 in the vicinity of the PEC cube introduces a large phase error which persists with distance and affects the solution of the $M3d_{24}$ scheme in the remaining region. In Figure 3b the use of the $M3d_{24}$ scheme in the whole region introduces errors in the amplitude and the phase due to using large stencils that intersect the PEC and using low resolution near the edges of the PEC. The result of applying the hybrid scheme, in which the Yee algorithm is applied with R=15 in the first two layers around the cube and the $M3d_{24}$ scheme is applied with R=5 in the remaining region, is shown in Figure 3c. It is seen that this hybrid scheme gives good accuracy in both the phase and the amplitude to a long distance.

The backscattered electric field versus distance from PEC spheres is shown in Figures 4 and 5, for spheres with diameters $D = 1.2\lambda$ and $D = 2.1\lambda$, respectively. The use of low resolution near the PEC sphere introduces a staircase error which can be reduced by using high resolution. It is seen from Figure 4a that the result of Yee algorithm with low resolution R=7 does not give accurate results in the vicinity of the sphere, and in addition a dispersion error appears with distance. In Figure 4b, the subgridding is used with the Yee algorithm such that, on the surface of the sphere and in two cells around the sphere, the Yee algorithm is applied with resolution R=21, and the same algorithm is applied with R=7 in the remaining region. The application of the Yee algorithm with high resolution in the vicinity of the sphere improves the results in this region, and the low resolution introduced a dispersion error in the remaining region, as seen in Figure 4b. This dispersion error is avoided by applying $M3d_{24}$ without increasing the resolution in that region to obtain the accurate results of Figure 4c. Similarly, it is seen from Figure 5 that the hybrid technique $M3d_{24}$-Yee with R=7/21 (the Yee algorithm is applied on the surface of the sphere and in two cells around the sphere), gives accurate results in amplitude and phase to long distance from the sphere.

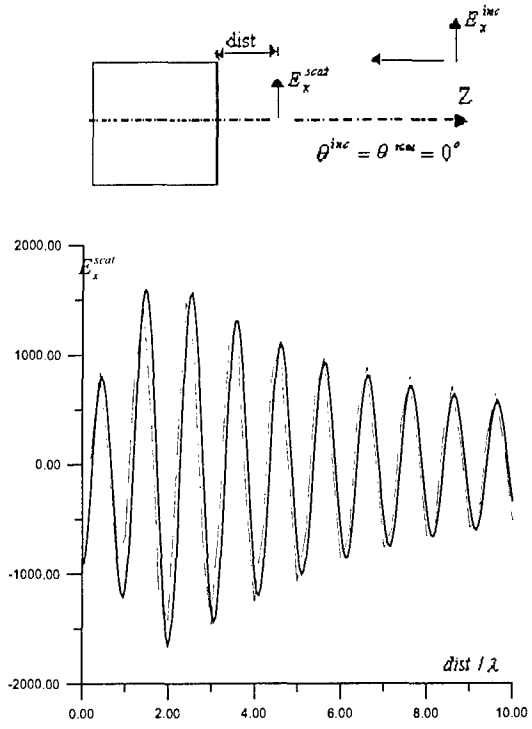

(a)

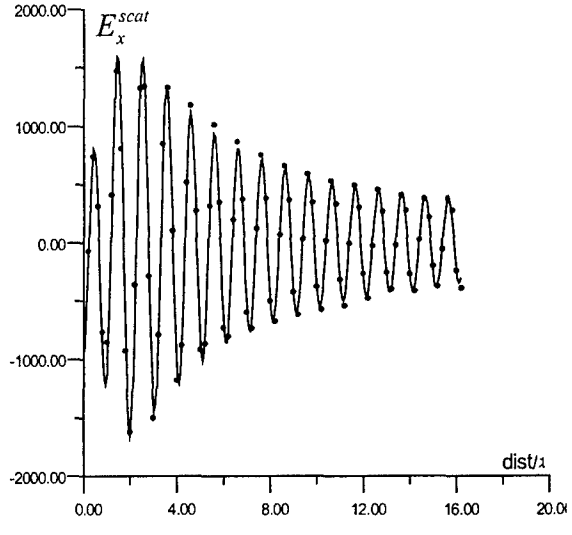

(b)

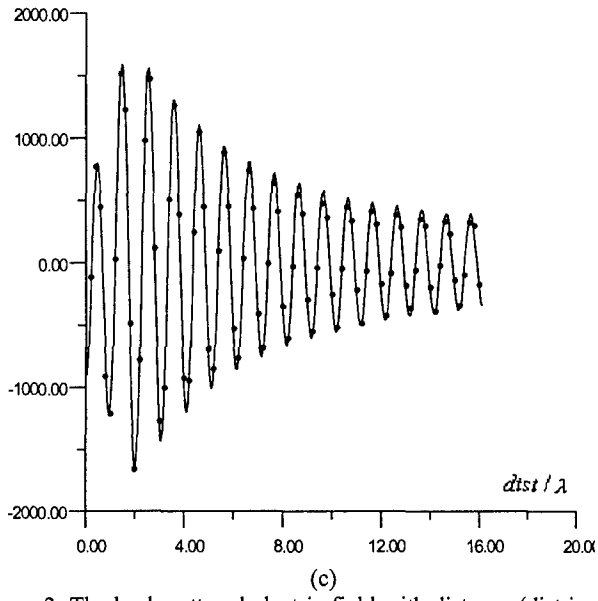

(c)

Figure 3. The backscattered electric field with distance (dist is the distance from the surface of the cube) for normal plane wave incidence on a cube (side length $L_x = L_y = L_z = 2.4\lambda$), $\overline{E}^{inc} = 1000\sin 2\pi f_0 t\ \hat{x}$, $f_0 = 900MHZ$,
———— Yee results (R=20).
(a) - - - - hybrid $M3d_{24}$-YEE with single resolution R=5, (b) $M3d_{24}$ with R=5 (dotted results), (c) hybrid $M3d_{24}$-YEE with sugridding R=5/15 (dotted results)

It is seen from Figures 3,4 and 5 that the electric field has reached the far region with high accuracy when using the $M3d_{24}$-Yee algorithm. Thereby this technique can be used to find directly the far-field, with a relatively small amount of memory, instead of using a near to far field transformation. The near to far field transformation [9] or [10] depends on calculating of the time derivative of the equivalent electric and magnetic currents which affect on the accuracy as shown in [10]. An improvement is achieved in [10] by implicitly calculating the required time derivatives of the equivalent electric and magnetic currents, instead of an explicit formulation of central differencing as in [9].

5. CONCLUSION

The direct application of 4th order FDTD algorithms in the vicinity of a perfect electric conductor (PEC) or dilectric scatterer introduces errors due to using large stencils in the 4th order algorithms. Other sources of error are the large variations of the fields in the vicinity of edges of a PEC or a large curvature of a surface of a PEC that can't be reproduced with a low resolution in the entire computational domain because of a large phase error due to the application of the Yee algorithm with low resolution. A hybrid $M3d_{24}$ - Yee scheme with subgridding has been used in the vicinity of the scatterer using a high-resolution grid and $M3d_{24}$ has been used with a

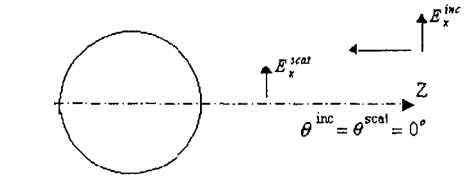

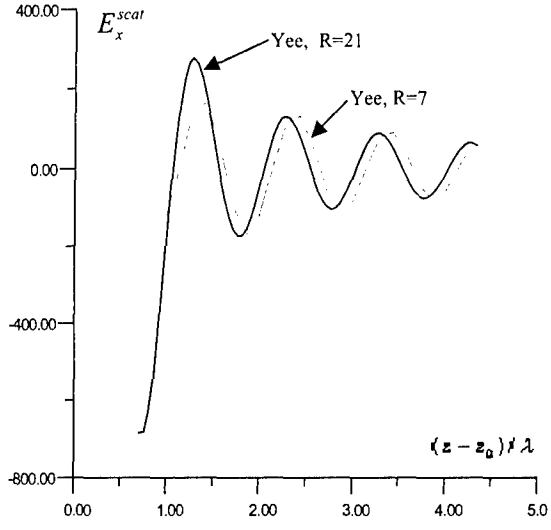

(a)

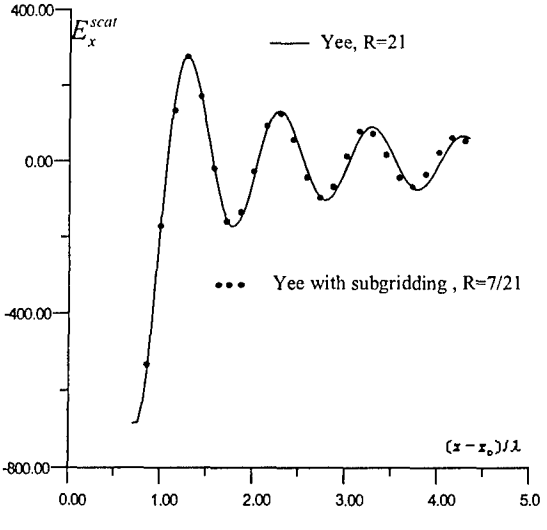

(b)

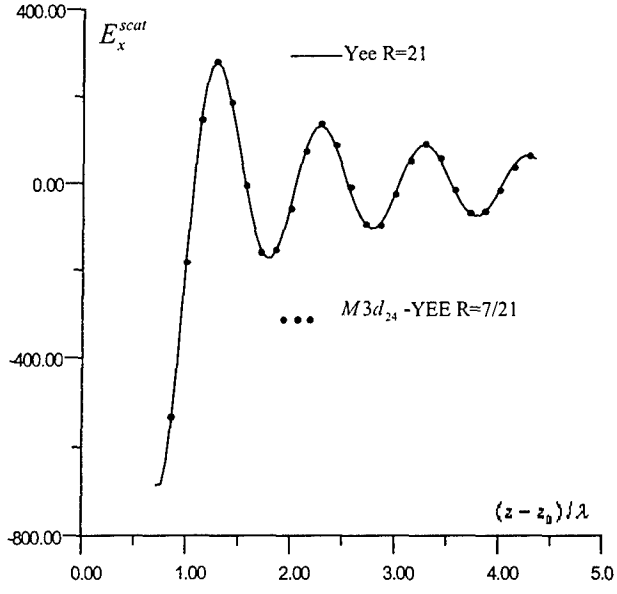

(c)

Figure 4. The scattered electric field E_x^{scat}, with distance, from a sphere with diameter 1.2λ. (x_0, y_0, z_0) is the center of the sphere, $\overline{E}^{inc} = 1000\sin 2\pi f_0 t\ \hat{x}$, $f_0 = 900MHZ$.

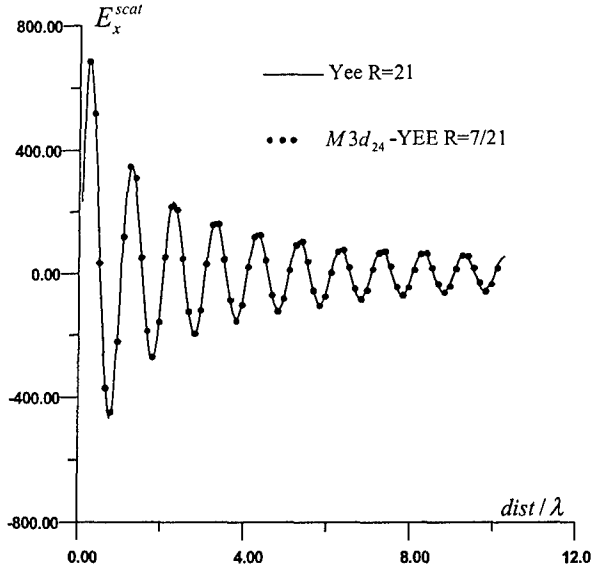

Figure 5. The scattered electric field with distance from the surface of a sphere with diameter 2.1λ, $\overline{E}^{inc} = 1000\sin 2\pi f_0 t\ \hat{x}$, $f_0 = 900MHZ$.

low-resolution grid in the other region. This scheme successfully overcomes the errors.

Using multi-resolution in the computational domain introduces a spurious reflection at the interface between the coarse grid and the fine one. A ratio of three has been used between the high-resolution grid and the low-resolution grid. The reflection coefficient of the subgridding of the present algorithm has been found to be below 47 dB for frequences corresponding to resolution greater than ten in the coarse grid.

Different test cases have been considered which showed the applicability of this hybrid scheme for different types of problems with low resolution. The scheme has been tested for scattering from PEC cubes and spheres. The scattering from a cube is a good test to show the applicability of the scheme in the vicinity of a PEC scatterer which contains edges. The field variation with distance, up to the far field region, shows the low dispersion error of the scheme. It has been found that the field reaches the far region for the test cases, with high accuracy, using as low resolution as R=5 with the present scheme, which on the other hand requires at least a resolution R=20 in the Yee algorithm. Such results suggest the use of this scheme to obtain the far field directly without the need to use near field to far field transformation.

6. REFERENCES

[1] Taflove, A (1995), Computational Electrodynamics The Finite-Difference Time-Domain Method, Artech House,Inc.

[2] Abd El-Raouf, H.E., El-Diwani, E.A., Ammar, A.A. and El-Hefnawi F.E. (March 1999), "A 3D modified FDTD (2,4) algorithm for improving phase accuracy with Low resolution," 16th National Radio Science Conference, NRSC'99,Ain Shams University, B4, Cairo-Egypt.

[3] Abd El-Raouf, H.E., El-Diwani, E.A., Ammar, A.A. and El-Hefnawi F.E. (July 1999), "A modified 3D fourth order FDTD algorithm $M3d_{24}$ for improving phase accuracy with low resolution,"IEEE Antennas and Propagation Society International Symposium, pp.196-199.

[4] Abd El-Raouf, H.E. (2000), Transient Radiation and Scattering of Electromagnetic Waves, Ph.D. Dissertation, Electrical Engineering Dept., Faculty of Engineering, Al-Azhar University.

[5] Hadi, M.F. (1996), A Modified FDTD (2,4) Scheme For Modeling Electrically Large Structures with High Phase Accuracy, Ph.D. Dissertation, ECEN Dept., University of Colorado, Boulder, CO.

[6] Hadi, M.F. and Piket-May, M. (1997), "A modified FDTD (2,4) scheme for modeling electrically large structures with high phase accuracy", IEEE Trans. Antennas and Propagation, Vol. AP-45, no.2, pp.254-264.

[7] Chevalier, M.W., Luebbers, R.J. and Cable, V.P. (1997), "FDTD local grid with material traverse," IEEE Trans.Antennas Propagat., Vol.45, pp.411-421.

[8] Okoniewski, M., Okoniewska, E. and Stuchly, M. (1997), "Three-dimensional subgridding algorithm for FDTD," IEEE Trans.Antennas Propagat., Vol.45 pp.422-429.

[9] Luebbers, J.R., Kunz.S.K., Schneider, M., and Hunsberger. (1991), "A finite-difference time-domain near zone to far zone transformation," IEEE Trans.Antennas Propagat., Vol.39 pp.429-433.

[10] Giannnopoulos, A., Randhawa, B.S., Tealby, J.M., and Marvin, A.C. (1997), "Modification to time domain near-field to far-field transformation for FDTD method," Electronics Letters, Vol.33 pp.2132-2133.